

Abstract

This paper describes submesoscale kinetic energy (KE) spectra and KE fluxes of coastal ocean currents observed from multiple platforms of satellite altimeters, shore-based high-frequency radars, and shipboard acoustic Doppler current profilers. One-dimensional wavenumber energy spectra of coastal currents decay with a slope of approximately k^{-2} at a wavenumber (k) of 0.5 km^{-1} . The spatial covariance of surface currents, equivalent to two-dimensional wavenumber spectra, has an anisotropic exponential shape with decorrelation length scales of $O(10)$ km close to the shore and $O(100)$ km offshore and principal axes nearly parallel with the shoreline, exhibiting coastal boundary effects on surface currents. The exponentially decaying spatial covariance function is consistent with submesoscale wavenumber spectra of a k^{-2} decay slope. Moreover, the KE fluxes of coastal surface currents show that zero-crossing wavenumbers, at which the forward and inverse cascades occur, appear at a length scale of $O(1)$ km and vary with time within a range of $O(1)$ km depending on the dominance of driving forces (e.g., tides and wind stress). The KE fluxes of statistically decomposed surface currents based on relationships between forcing and responses in the frequency domain exhibit unique separation length scales (inverse of zero-crossing wavenumbers) of $O(1)$ km and reflect the characteristics of the responses to individual forcing and their interactions at all spatial scales.

Data Analysis

The HFR-derived hourly surface currents with 1, 6, and 20 km spatial resolutions off the U.S. West Coast (USWC) over two years (2008 to 2009) are analyzed [e.g., [1]]. The HFR surface currents contain various aspects of coastal surface circulation averaged over upper one meter depth including poleward- or equatorward-propagating signals near the coast, near-inertial oscillations, surface tide-coherent currents, local and remote wind-forced circulation, intermittent and persistent submesoscale and mesoscale eddies, and surface modulations due to internal waves and tides.

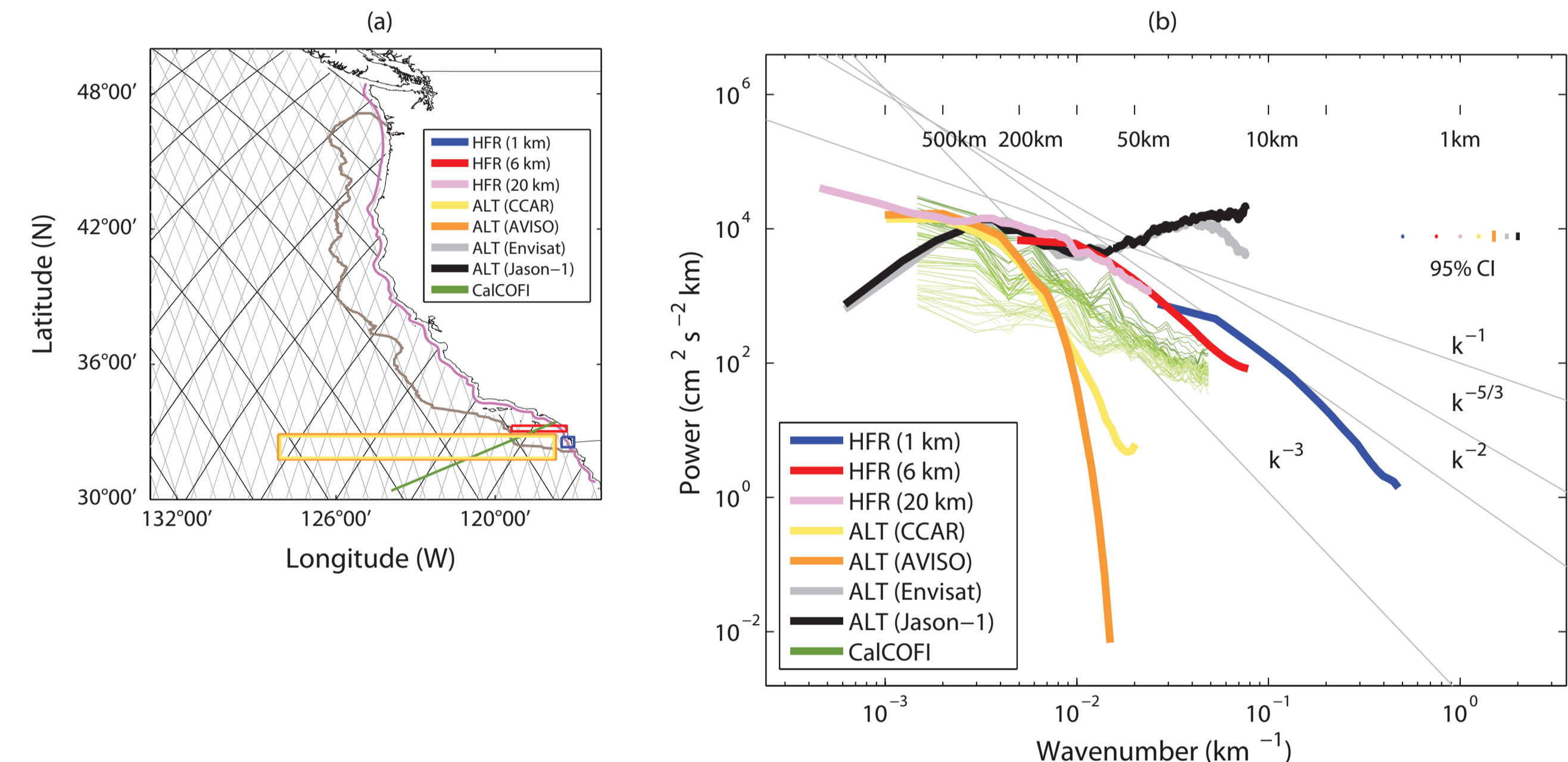


Figure 1: A study domain for continuity of ocean surface scales off the USWC. Sampling locations of HFR surface currents with three spatial resolutions (1, 6, and 20 km), ALT gridded geostrophic currents (CCAR and AVISO), ALT along-track SSHAs (Envisat and Jason-1), and a CalCOFI cruise track (Line 90) are indicated. The effective coverage of HFR surface currents is denoted by a dark gray curve. (b) and (c): Power spectra of high-frequency radar-derived (HFR; 1, 6, and 20 km resolutions) surface currents and altimeter-derived geostrophic currents [ALT; optimally interpolated current products of CCAR (~25 km resolution) and AVISO (~33 km resolution) and along-track Envisat and Jason-1] for two years (2007 and 2008) in the (b) wave-number domain [Length scales (L) of 1, 5, 10, 50, 100, 200, 500, and 1000 km are marked] and (c) frequency domains [Six seasonal harmonics (SA_1 to SA_6), spring-neap (SN , 14.765-day), lunar fortnightly (LF , 13.661-day), S_1 , K_1 , M_2 , and S_2 tidal frequencies are marked]. The wave-number spectra of shipboard ADCP currents in quarterly CalCOFI cruises (1993 to 2004) in vertical are shown as light green (shallow; at 16 m depth) to dark green (deep, 408 m depth) curves.

Four kinds of products of ALT-derived geostrophic currents in the northeastern Pacific (30°N to 50°N, 114°W to 133°W) are examined (Figure 1a). Two sets of 7-daily along-track sea surface height anomalies (SSHAs) with respect to the seven-year mean dynamic topography from Envisat and Jason-1 are analyzed. Two gridded products of the Colorado Center for Astrodynamics Research (CCAR) daily geostrophic currents with a quarter degree resolution and the AVISO 7-daily geostrophic currents with approximately one-third degree resolution are considered.

Subsurface currents observed from the shipboard ADCP in quarterly California Cooperative Fisheries Investigation (CalCOFI) cruises for 12 years (1993 to 2004) are analyzed. Although this data set is not overlapped with HFR and ALT data, it will provide typical energy spectra of subsurface currents.

Energy Spectra

The one-dimensional wavenumber spectra of HFR surface currents at three spatial resolutions (1, 6, and 20 km) show consistent and continuous energy distribution ranging from $O(1000)$ km to $O(1)$ km. Most of them decay with k^{-2} at high wavenumber in agreement with typical submesoscale energy spectra (Figure 1b). While driving forces of circulation and partitioning of both geostrophic and ageostrophic components may vary regionally and appear in energy spectra, the estimated energy spectra have a robust k^{-2} behavior. The energy spectra of ALT cross-track currents at scales larger than 100 km ($L > 100$ km) agree with those of HFR surface currents and show observational limits of present-day satellite ALT at scales below 100 km scale. As the HFR surface currents off southern California contain a minimum ageostrophic currents (e.g., wind-driven components), their power spectra are comparable to the spectra of ALT cross-track geostrophic currents (Envisat and Jason-1) (Figure 1b). The variance difference at low wavenumber ($L > 500$ km) in the HFR and along-track ALT observations results from existence of alongshore signals with large wavelength near the coast (e.g., coastally trapped waves). As HFR surface currents were sampled in the cross-shore (1 and 6 km resolutions) and along-shore directions (20 km resolution), the energy spectra may contain coastal boundary effects due to bathymetry and shoreline. The one-dimensional wavenumber spectrum with a slope of k^{-2} (or two-dimensional wavenumber spectrum with a slope of k^{-3}) is related to the exponential covariance function in the physical space.

Energy spectra of subsurface currents along the CalCOFI Line 90 show a continuous transition from mesoscale to submesoscale oceanic energy and their vertical structures (Figure 1b). The energy spectrum at a depth of 16 m and 408 m is de-

noted by a curve with dark green and light green, respectively. Energy spectra of near-surface currents (upper 60 m) have k^{-1} ($L > 150$ km) and k^{-2} ($L \leq 150$ km) slopes that bend at a scale of 150 km.

Energy Fluxes

As an example, KE fluxes [$\Pi(k)$] are estimated from surface current maps obtained from HFRs off the southern San Diego coast over a wind-dominant period (1-km resolution; Figure 2a). Submesoscale features are visible as an approximately 10-km radius eddy (Figure 2a). The zero-crossing wavenumbers of the estimated KE fluxes appear between 0.06 km^{-1} and 0.1 km^{-1} , corresponding to the separation length scales of 10 km and 15 km (Figure 2b). Note that a separation length scale (δ) denotes an inverse of the zero-crossing wavenumber (κ).

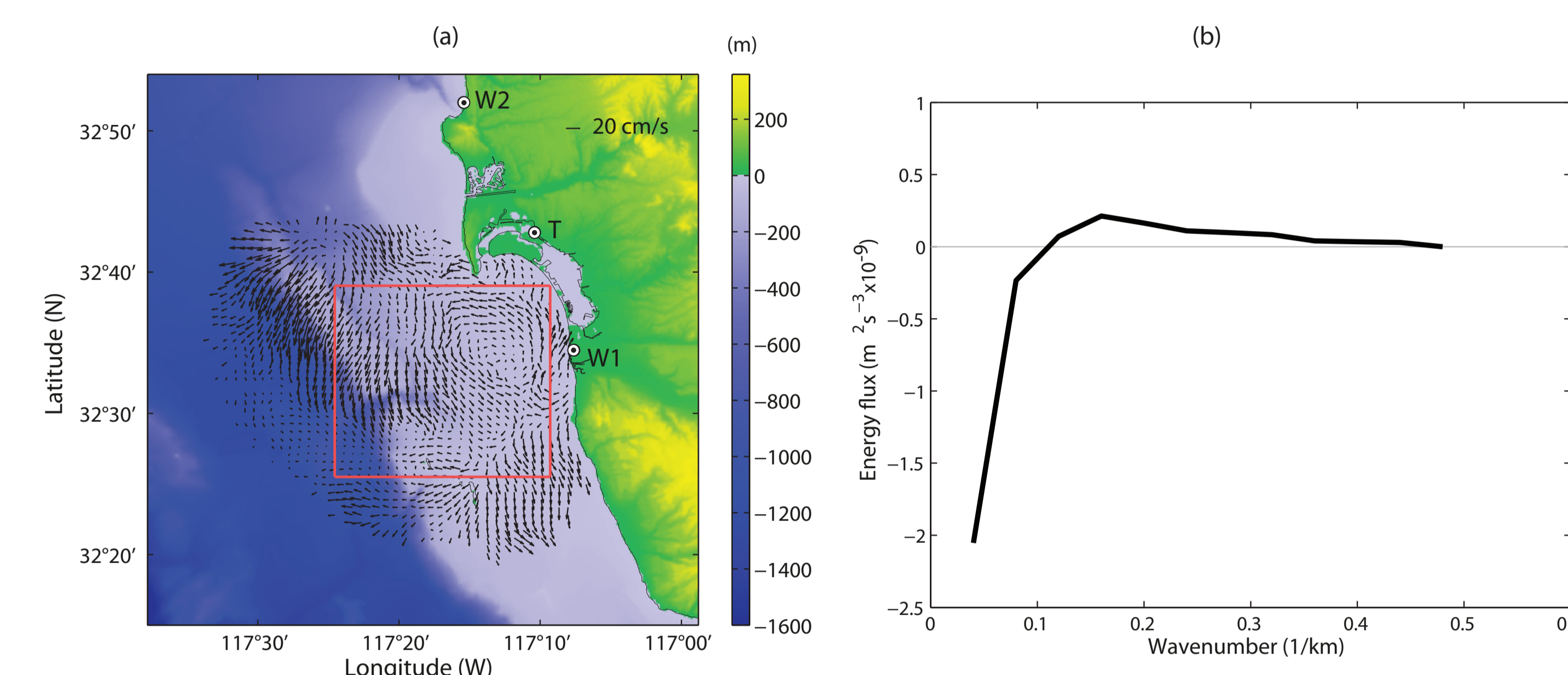


Figure 2: (a): Surface current maps obtained from HFRs off the southern San Diego coast (1-km spatial resolution). (b) KE fluxes [$\Pi(k)$] estimated from data within a red box in Figures 2a.

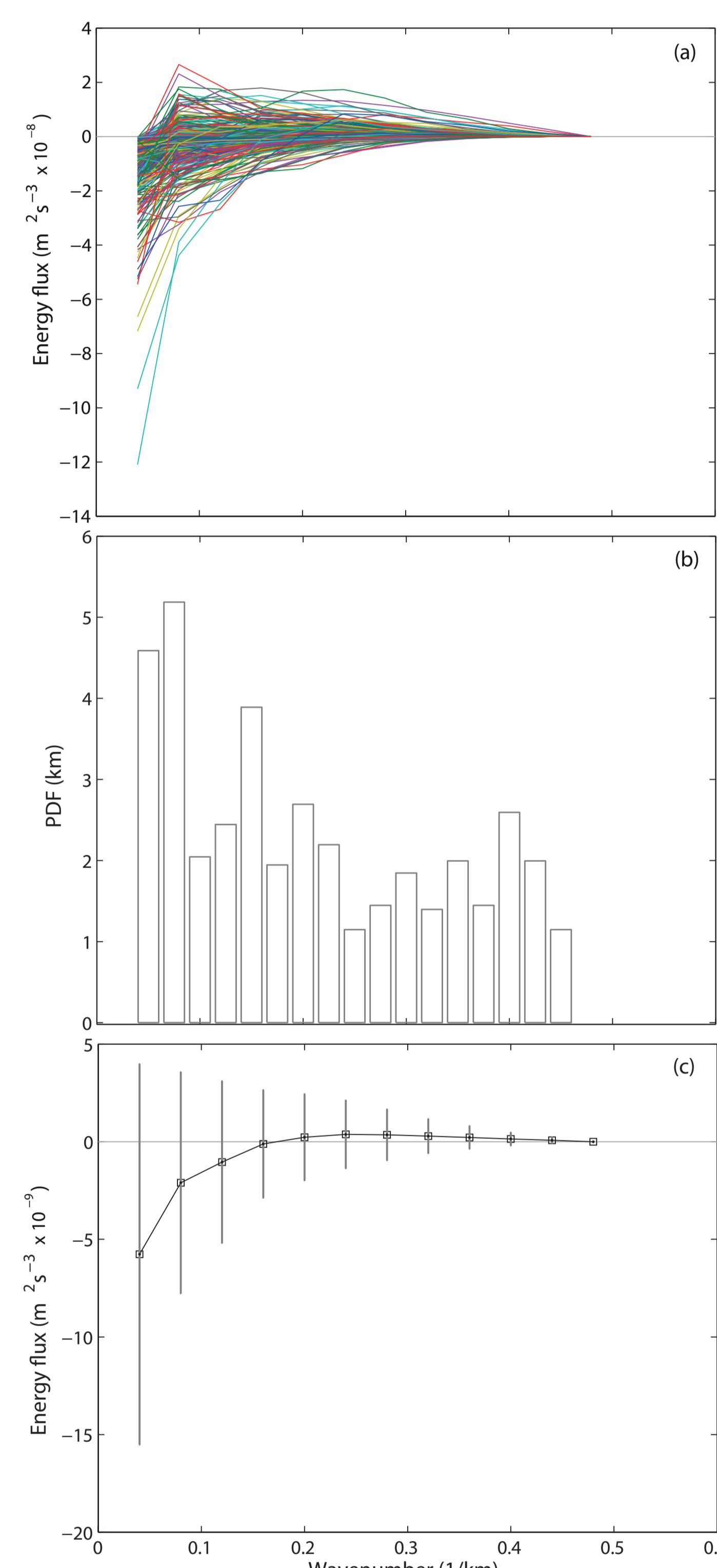


Figure 3: KE fluxes [$\Pi(k)$] estimated from hourly surface current maps at a 1-km spatial resolution off the coast of southern San Diego over a period of six years (2003 to 2009). (a) Conditionally selected KE fluxes. (b) A probability density function (PDF) of zero-crossing wavenumbers of the conditionally selected KE fluxes. (c) Mean (square) and standard deviation (error bar) of conditionally selected and averaged KE fluxes for each wavenumber bin [$\Pi(k)$].

Six hourly ensemble averaged KE fluxes, estimated from hourly surface current maps over a period of six years (2003 to 2009; 8,772 realizations), are conditionally selected (Figure 3a; $M = 843$; 9% of total realizations). A PDF of zero-crossing wavenumbers of conditionally selected KE fluxes shows that the separation length scales are concentrated at a scale longer than 5 km (Figure 3b). The bin-averaged KE flux in the wavenumber domain (Figure 3c) shows a zero-crossing wavenumber of 0.2 km^{-1} , i.e., a separation length scale of $O(1)$ km.

The KE flux time series at each wavenumber, estimated from hourly HFR-derived surface current maps, are shown with the time series of concurrent observations of local winds [Tijuana River (TJR; W1) and Scripps Pier (SIO; W2)] and surface tides [San Diego Bay (SDB; T)] over a period of one month (February, 2004) off the coast of southern San Diego to examine their influence on the KE fluxes and to present the temporal variation in separation length scales depending on the oceanic forcing and responses (Figure 4).

Four time periods in which these primary drivers are significant and all positive KE fluxes are chosen (time windows marked as A to D in Figure 4). The KE fluxes estimated from HFR-derived surface currents are more influenced by tides than winds because winds can be more intermittent and their high-frequency fluctuations typically occur under windy conditions (B and D in Figures 4). In the time period of C, the KE fluxes are all positive because of (1) an absence of large-scale motions under both weak winds and tides or (2) an existence of the separation length scale longer than 25 km. Although the local winds and spring tide conditions during A and A' are similar, the magnitude of spatially averaged surface currents is more enhanced during A than A', which might result from constructive interactions among spring tide, M_2 tide, and winds. Thus, the separation length scales of the KE fluxes during A tend to appear clearly at a range of $O(1)$ km.

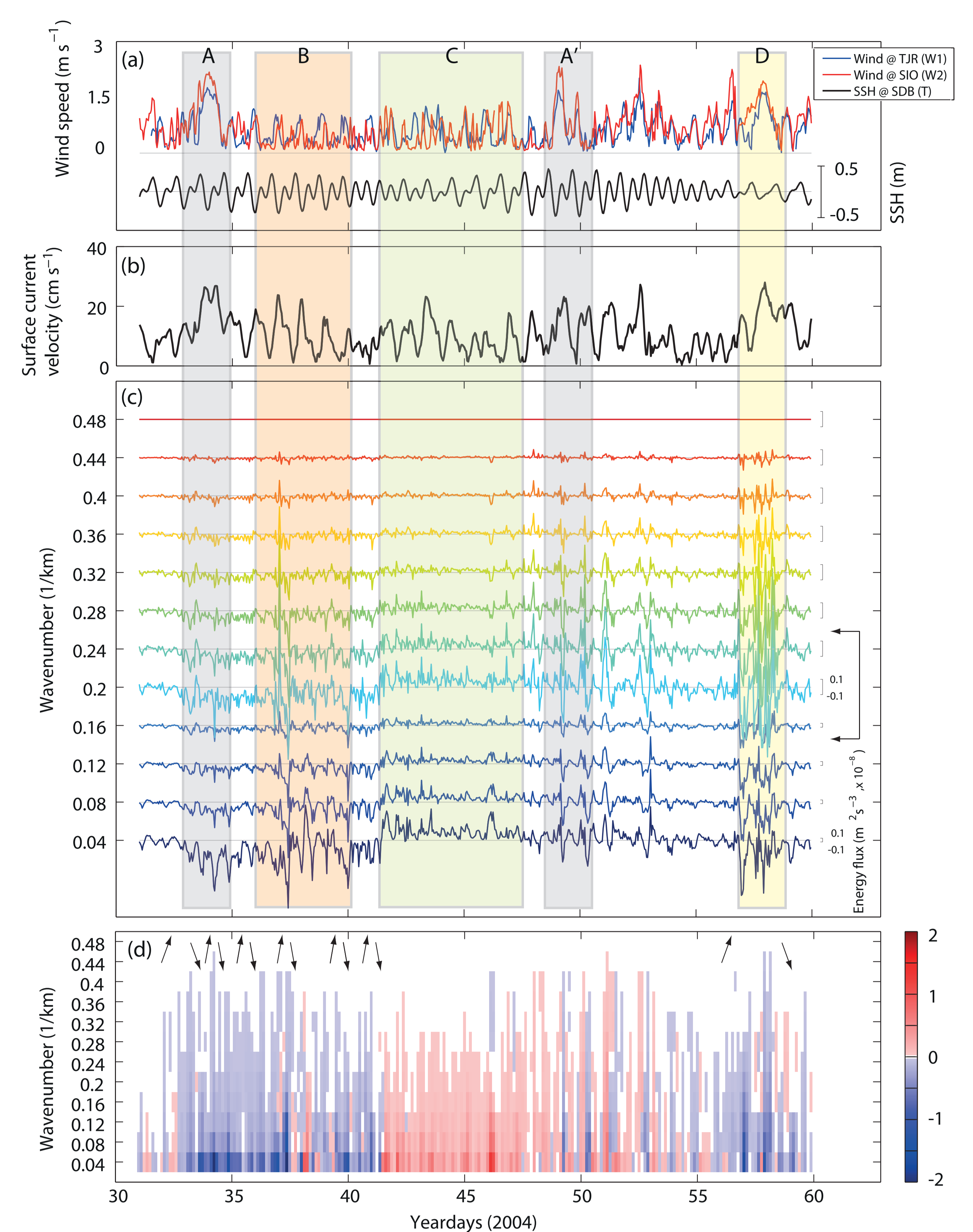


Figure 4: (a) Hourly time series of local winds at Tijuana River Valley (TJR; W1) and Scripps Pier (SIO; W2) and sea surface elevation at San Diego Bay (SDB; T) (Figure 2a). (b) Hourly time series of spatially averaged HFR-derived surface currents within a red box (Figure 2a). (c) Time series of KE fluxes at each wavenumber [$\Pi(k, t)$] estimated from HFR-derived surface currents within a red box (Figure 2a). Time series of KE fluxes at each wavenumber is color-coded and scaled with two constants, 5×10^7 ($k < 0.2 \text{ km}^{-1}$) and 2×10^8 ($k \geq 0.2 \text{ km}^{-1}$). Note that all time series of KE fluxes in Figure 4c are in an identical range of $\pm 0.1 \times 10^{-8}$. Both strong winds and spring tide (A and A'), spring tide only (B), positive KE fluxes at low wavenumber (C), and enhanced fluctuations of KE fluxes with local wind dominance (D) are marked. (d) Temporal variation in the zero-crossing wavenumber (κ) of KE fluxes [$\Pi(k, t)$; $\text{m}^2 \text{ s}^{-2}$]. Positive and negative values of KE fluxes are denoted with red and blue, respectively, and temporal moving directions of the zero-crossing wavenumber in the wavenumber domain are marked with black arrows.

The zero-crossing wavenumbers (white areas in Figure 4d) of the KE flux time series appear between 0.12 km^{-1} and 0.28 km^{-1} , i.e., separation length scales of 4 km and 9 km, respectively (black arrow-bracket in Figure 4c), which indicates that the KE fluxes propagate into larger or smaller length scales (black arrows in Figure 4d) depending on the magnitude of primary geophysical drivers and their interactions.

Conclusion

Submesoscale oceanic energy spectra are examined with currents observed from multiple platforms, including satellite ALT, shore-based HFRs, and shipboard ADCPs. The one-dimensional wavenumber energy spectra of coastal currents agree with those of ALT-derived cross-track currents at scales exceeding 100 km and decay with a slope of approximately k^{-2} at a wavenumber of 0.5 km^{-1} . Moreover, subsurface currents obtained from shipboard ADCPs support the continuous transition of oceanic energy spectra between mesoscale and submesoscale. The spatial covariance functions of surface currents, equivalent to two-dimensional wavenumber spectra, exhibit coastal boundary effects on surface currents: an anisotropic exponential shape with decorrelation length scales of $O(10)$ km close to the shore and $O(100)$ km offshore and principal axes nearly parallel with the shoreline. The exponentially decaying spatial covariance function is consistent with submesoscale one-dimensional wavenumber spectra of a k^{-2} decay behavior. The submesoscale oceanic KE fluxes of coastal surface currents show that zero-crossing wavenumbers, where the inverse and forward cascades occur, appear at a length scale of $O(1)$ km and vary with time between 4 km and 9 km depending on the dominance of tides and wind stress. The KE fluxes of decomposed surface currents by using statistical relationships between forcing and responses in the frequency domain exhibit unique separation length scales, reflecting the characteristics of responses to individual forcing and their interactions at all spatial scales. In this paper the separation length scales of the decomposed surface currents and their order are quantified based purely on observations, which can be the significance of this work.

Acknowledgement

Sung Yong Kim is supported by the Basic Science Research Program through the National Research Foundation (NRF), Ministry of Education (NRF-2013R1A1A2057849), Republic of Korea. Surface current data are provided by the universities and research organizations on the USWC: SIO, USC, UCSB, CalPoly, NPS, SFSU, HSU, UCD. The altimeter products were produced by SSALTO/DUACS and distributed by AVISO with support from CNES. The altimeter-derived geostrophic current data were obtained from the Colorado Center for Astrodynamics Research.

References

- [1] S. Y. Kim, E. J. Terrill, B. D. Cornuelle, B. Jones, L. Washburn, M. A. Moline, J. D. Paduan, N. Garfield, J. L. Largier, G. Crawford, and P. M. Kosro. Mapping the U.S. West Coast surface circulation: A multiyear analysis of high-frequency radar observations. *J. Geophys. Res.*, 116, 2011.